Design proposal of Mach Zehnder Interferometer on a Silicon Photonics Platform

Viveka B Raghu
vivekabr97@gmail.com

***Abstract*—Interferometers are important devices for data communications and for switching in Silicon Photonics. Mach Zehnder Interferometer (MZI) is among the important interferometers for dynamic control of optical signals for routing and switching in optical networks. This document explores the design of the Mach Zehnder Interferometer.**

Keywords—Mach Zehnder, optical network

Introduction

Silicon Photonics is a rapidly growing field and indispensable for the growth of AI. Without Silicon photonics it is not possible to catch up with the bandwidth requirements of AI applications and future networks. The silicon photonic transciever device consists of active and also passive devices such as grating couplers, modulators , lasers and detectors. Modulators are the devices that convert data encoded in electrical signals into optical signals. Mach Zehnder Interferometer is an important type of modulator that does this conversion and is achieved by controlling the intensity of optical signals as a result of interference.

I. THEORY OF MZI

The Mach-Zehnder Interferometer is a device that achieves interference between optical signals that have traversed different lengths of waveguides that results in a phase shift between the signals.

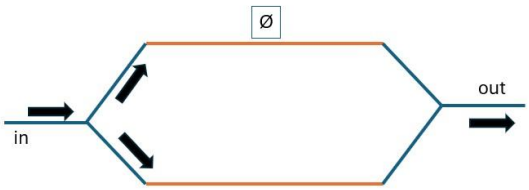

Fig.1. Schematic of MZI

The input light splits into two different paths whose fields can be represented as E1 and E2. They travel through two parallel waveguides which may be of slightly different lengths and thus undergo a phase shift. The phase shifted light interferes at the output port. The propagation constants for the signals can be represented by ß1 and ß2 respectively. Before interference at the output port the optical fields can be represented as

$$Eo1 = E1(e)^{-i\text{ß}1L1-(\alpha1/2)L1} = \frac{Ei}{\sqrt{2}}e^{-i\text{ß}1L1-(\alpha1/2)L1} \quad (1)$$

$$Eo2 = E2(e)^{-i\text{ß}2L2-(\alpha2/2)L2} = \frac{Ei}{\sqrt{2}}e^{-i\text{ß}2L2-(\alpha2/2)L2} \quad (2)$$

The output can be mathematically represented by:

$$Eo = Eo1 + Eo2 \quad (3)$$

$$Eo = \frac{1}{\sqrt{2}}(Eo1 + Eo2) \quad (4)$$

Upon substitution, the final expression becomes

$$Eo = \frac{Ei}{2}\left(e^{-i\text{ß}1L1-(\alpha1/2)L1} + e^{-i\text{ß}2L2-(\alpha2/2)L2}\right) \quad (5)$$

The output intensity becomes

$$Io = \frac{Ii}{4}\left|e^{-i\text{ß}1L1-(\alpha1/2)L1} + e^{-i\text{ß}2L2-(\alpha2/2)L2}\right|^2 \quad (6)$$

For lossless waveguides, α1 and α2 = 0 which simplifies the above expression as follows

$$Io = \frac{Ii}{2}[1 + \cos(\text{ß}1L1 - \text{ß}2L2)] \quad (7)$$

For a balanced interferometer the above equation becomes

$$Io = \frac{Ii}{2}[1 + \cos(\Delta\text{ß}L)] \quad (8)$$

For an imbalanced interferometer the equation becomes

$$Io = \frac{Ii}{2}[1 + \cos(\text{ß}\Delta L)] \quad (9)$$

Equations (8) and (9) are also termed as transfer function equations of the interferometer. Plotting Eq (9) we get

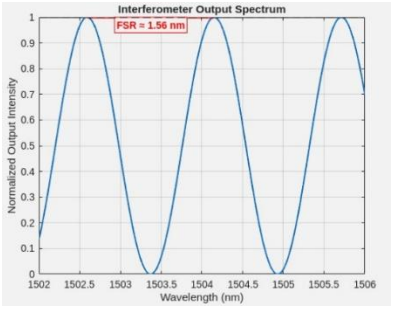

Fig.2. Plot of transfer function

II. SIMULATION

Several modes exist within the waveguides that are solutions to the maxwell's equations. This MZI design specifically is based on the TE mode with a simulated profile as shown below.

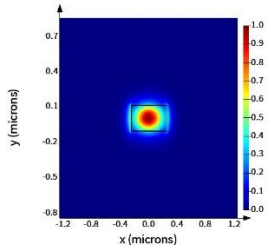

Fig.3. Field distribution of TE mode

Some of the other modes are as shown in the image below.

mode #	effective index	wavelength (μm)	loss (dB/cm)
1	2.444988+1.248107e-09i	1.55	0.00043945
2	1.770662+8.509426e-10i	1.55	0.00029961
3	1.494231+4.974653e-10i	1.55	0.00017516
4	1.346613+2.152209e-10i	1.55	7.5779e-05
5	1.345073+2.892314e-10i	1.55	0.00010184

Fig.4. Modes within waveguide

The waveguide offers different effective index for different modes. This is because each mode is seen as an eigen state within the waveguide with a unique propagation constant and effective index is described by

$$n\_eff = \frac{ß}{k} \qquad (10)$$

For the waveguide used in this design , the variation of effective index with wavelength is according to the graph shown below.

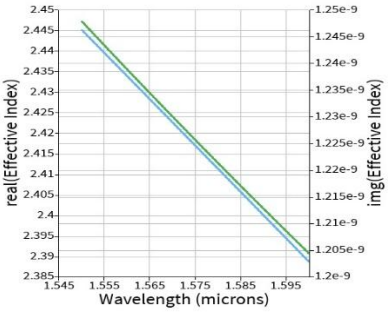

Fig.5.Plot of effective index vs wavelength

The equation that mathematically describes n_eff as a function of wavelength is obtained from fitting the points of effective index against the wavelength.

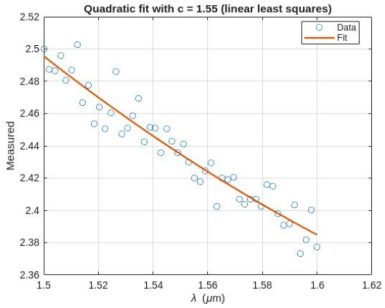

Fig.6. Quadratic fit of index VS wavelength

$$n_{eff} = 2.44 - 1.13 * (\lambda - 1.55) - 0.04 * (\lambda - 1.55)^2 \quad (11)$$

It is also to be noted that information that is encoded on optical signals travels as an envelope within the waveguide with group velocity and experiences the group index . For the waveguide used in this design the variation of group index with wavelength is as shown in the plot below.

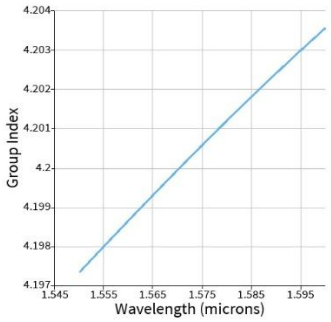

Fig.7. Plot of group index vs wavelength

A. Interferometer simulated on Lumerical interconnect:

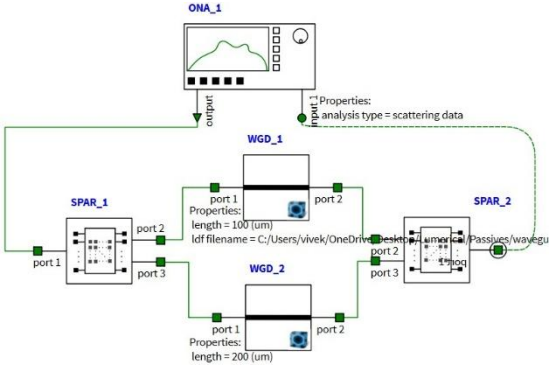

Fig.8. Interferometer setup on Lumerical Interconnect

The interferometer setup on interconnect is made as shown in the image above. There is an optical network analyzer from which the input is connected to the y-branch. One of the outputs of the y-branch is connected to the waveguide of length 100 microns. The output of the first waveguide is connected to the first port of the output y-branch. The output from the second port of the input y-branch is connected to the input port of the second waveguide and the output of the second waveguide is connected to the second input port of the output y-branch. The output of the y-branch is fed as input to the optical network analyzer. It is to be noted that the interferometer simulated above is an imbalanced interferometer.

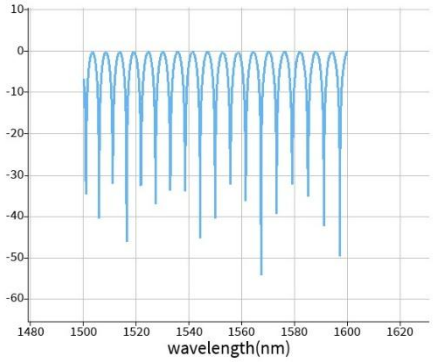

Fig.9. Interferometer transmission in (db) VS wavelength

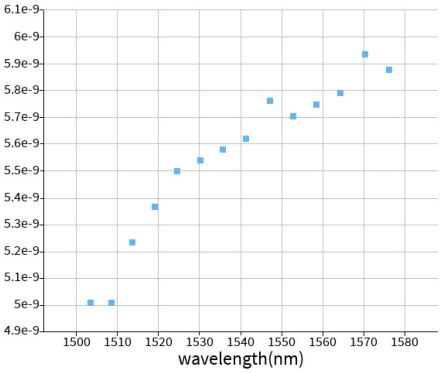

Fig.10. Interferometer FSR VS wavelength

Proposed layout to be fabricated on the Silicon chip of dimensions 605µm (Width) and 410µm (Height) is as shown below.

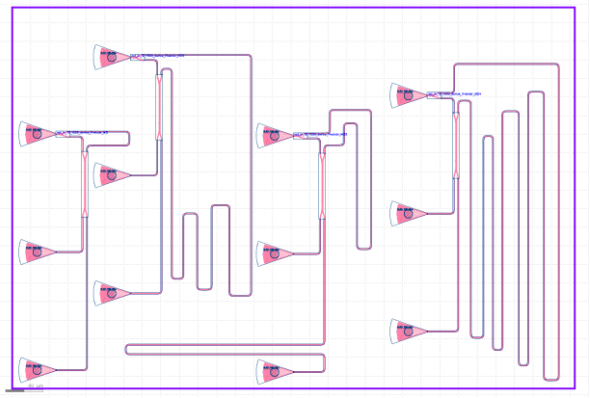

Fig.11. K-layout based interferometer layout

The layout above was created using K-Layout with the latest version of SiEPIC PDK that has the components predefined.

Effect of fabrication variation:
Corner Analysis

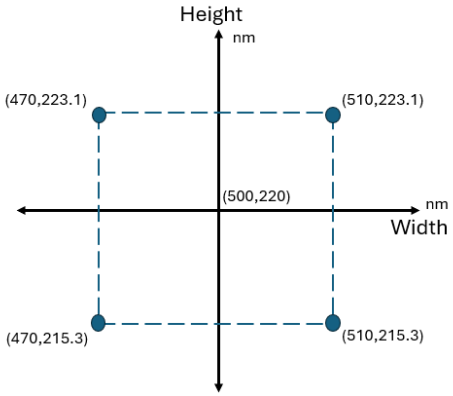

Fig.12. Coordinates of corner analysis.

To be able to predict device performance under conditions where variations are introduced in fabrication, four extreme cases are considered apart from the ideal waveguide dimensions (width = 500 nm, height = 220 nm).
Lumerical mode simulations were performed for each of these cases. Trends in effective index and group index with respect to wavelength was plotted.

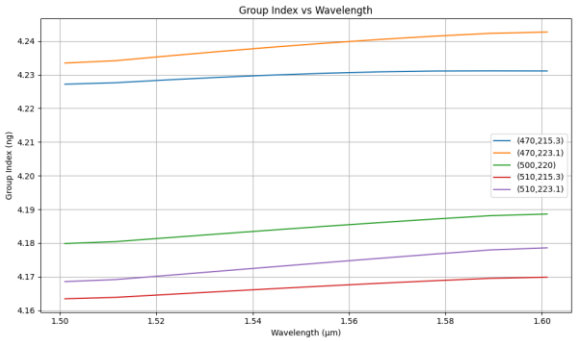

Fig.13. Corner analysis simulations (ng VS wavelength)

A.Experimental measurement results and analysis.

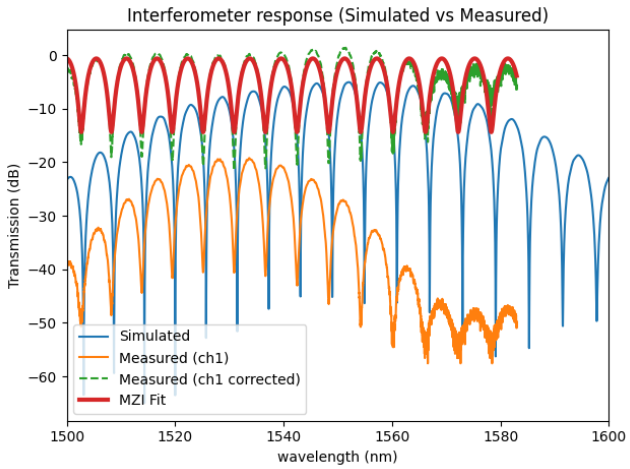

Fig.14. Experimental results VS simulations

The Mach Zehnder interferometers were fabricated according to the k-layout based design and was measured. The figure above is the response from the first interferometer of path length difference $\Delta l = 100$ µm.
Baseline correction was performed on the measured data to remove the baseline shape of grating couplers. The baseline corrected data was curve fitted from which measured group index and free spectral range were determined. It is to be noted that the fitted parameters from the measurement results are [2.3826, -1.109, 0.0234] . The comparison of theoretical variation of group index VS measured variation of group index as a function of wavelength is as shown in the figure below.

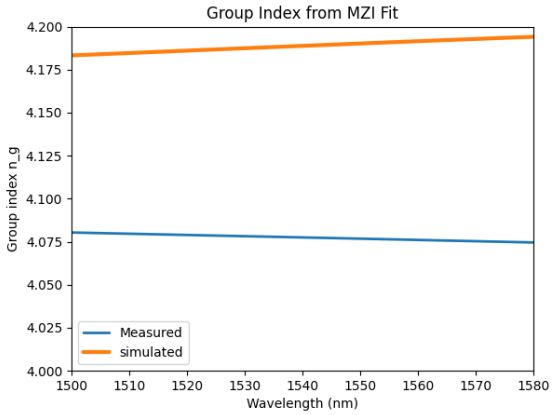

Fig.15. Measured group index VS simulated group index

The measured group index against the other points of corner analysis is as shown in the figure below.

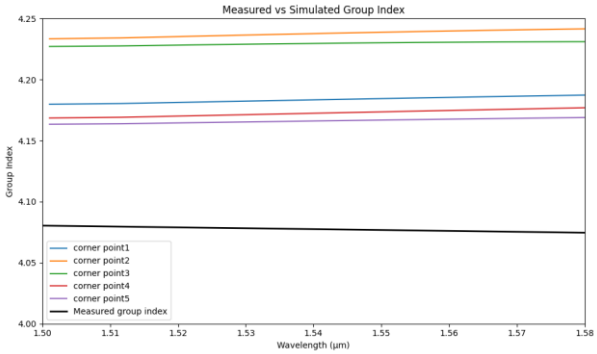

Fig.16. Measured group index VS corner analysis results

The measured group index is out of the bounds of the simulated corner points, the free spectral range (FSR) is well within the bounds of the simulated corner points. The measured FSR from experimental data is 5.735nm against the predicted value of 5.77 from corner analysis. The measured mean group index is at 4.078 which is out of bounds of corner analysis.

Conclusions

To summarize, we have conceptualized the Mach Zehnder Interferometer, come up with theoretical models for interferometer transfer function and also demonstrated through lumerical simulations the modes of the waveguide, field distribution and transmission spectrum. The design has been fabricated and measured . We have extracted parameters of interest from curve fitting the experimental data. We have observed that there is a high degree of similarity in performance of the fabricated interferometer compared to the design simulations.

ACKNOWLEDGMENT

I would like to acknowledge that the silicon photonics design course offered on EdX by Professor Lukas Chrostowski of University of British Columbia has been a very useful value addition in the field of photonics. The course is well structured and accelerates learning by deep thinking through assignments. I would also like to sincerely thank the teaching assistant for his help throughout the course on matters related to assignments submissions software and other related issues.

REFERENCES

[1] A. Liu et al., “A high-speed silicon optical modulator based on a metal-oxide-semiconductor capacitor,” *Nature* 427, 615–618 (2004).

[2] L. Liao et al., “High-speed silicon Mach–Zehnder modulator,” *Optics Express* 13(8), 3129–3135 (2005).

[3] W. M. J. Green, M. J. Rooks, L. Sekaric, Y. A. Vlasov, “Ultra-compact, low RF power, 10 Gb/s silicon Mach–Zehnder modulator,” *Optics Express* 15(25), 17106–17113 (2007).

[4] R. Soref, “The past, present, and future of silicon photonics,” *IEEE J. Sel. Top. Quantum Electron.* 12(6), 1678–1687 (2006).

[5] G. Yurtsever et al., “Photonic integrated Mach–Zehnder interferometer with an …” (application paper / review), *Scientific Reports / PMC* (2014).

[6] L. Chrostowski and M. Hochberg, *Silicon Photonics Design: From Devices to Systems*. Cambridge University Press, 2015.